

# Patterned Gene Expression Directs Bipolar Planar Polarity in *Drosophila*

Jennifer A. Zallen\* and Eric Wieschaus

Department of Molecular Biology  
Princeton University  
Lewis Thomas Lab  
Washington Road  
Princeton, New Jersey 08544

## Summary

During convergent extension in *Drosophila*, polarized cell movements cause the germband to narrow along the dorsal-ventral (D-V) axis and more than double in length along the anterior-posterior (A-P) axis. This tissue remodeling requires the correct patterning of gene expression along the A-P axis, perpendicular to the direction of cell movement. Here, we demonstrate that A-P patterning information results in the polarized localization of cortical proteins in intercalating cells. In particular, cell fate differences conferred by striped expression of the *even-skipped* and *runt* pair-rule genes are both necessary and sufficient to orient planar polarity. This polarity consists of an enrichment of nonmuscle myosin II at A-P cell borders and Bazooka/PAR-3 protein at the reciprocal D-V cell borders. Moreover, *bazooka* mutants are defective for germband extension. These results indicate that spatial patterns of gene expression coordinate planar polarity across a multicellular population through the localized distribution of proteins required for cell movement.

## Introduction

Many properties of body structure are established through the reorganization of cell populations, where small shifts in the position of individual cells collectively generate a global change in tissue morphology. Tissue remodeling involves the coordination of multiple cellular processes—including intercellular communication, polarized cell motility, and selective adhesion—across a three-dimensional population of cells. In particular, the conserved process of convergent extension drives axis elongation, gastrulation movements, and organogenesis in both vertebrates and invertebrates (Keller et al., 2000; Keller, 2002; Tada et al., 2002; Wallingford et al., 2002).

During convergent extension in the gastrulating *Drosophila* embryo, cells of the germband ectoderm intercalate along the dorsal-ventral (D-V) axis, causing the germband to more than double in length along the anterior-posterior (A-P) axis (Campos-Ortega and Hartenstein, 1985). This multicellular reorganization can occur in the absence of cell division (Edgar and O'Farrell, 1989) and significant cell shape changes (Irvine and Wieschaus, 1994), indicating that it is driven by cell rearrangement. While cell migrations are aligned along the D-V axis, polarized intercalation persists in mutants

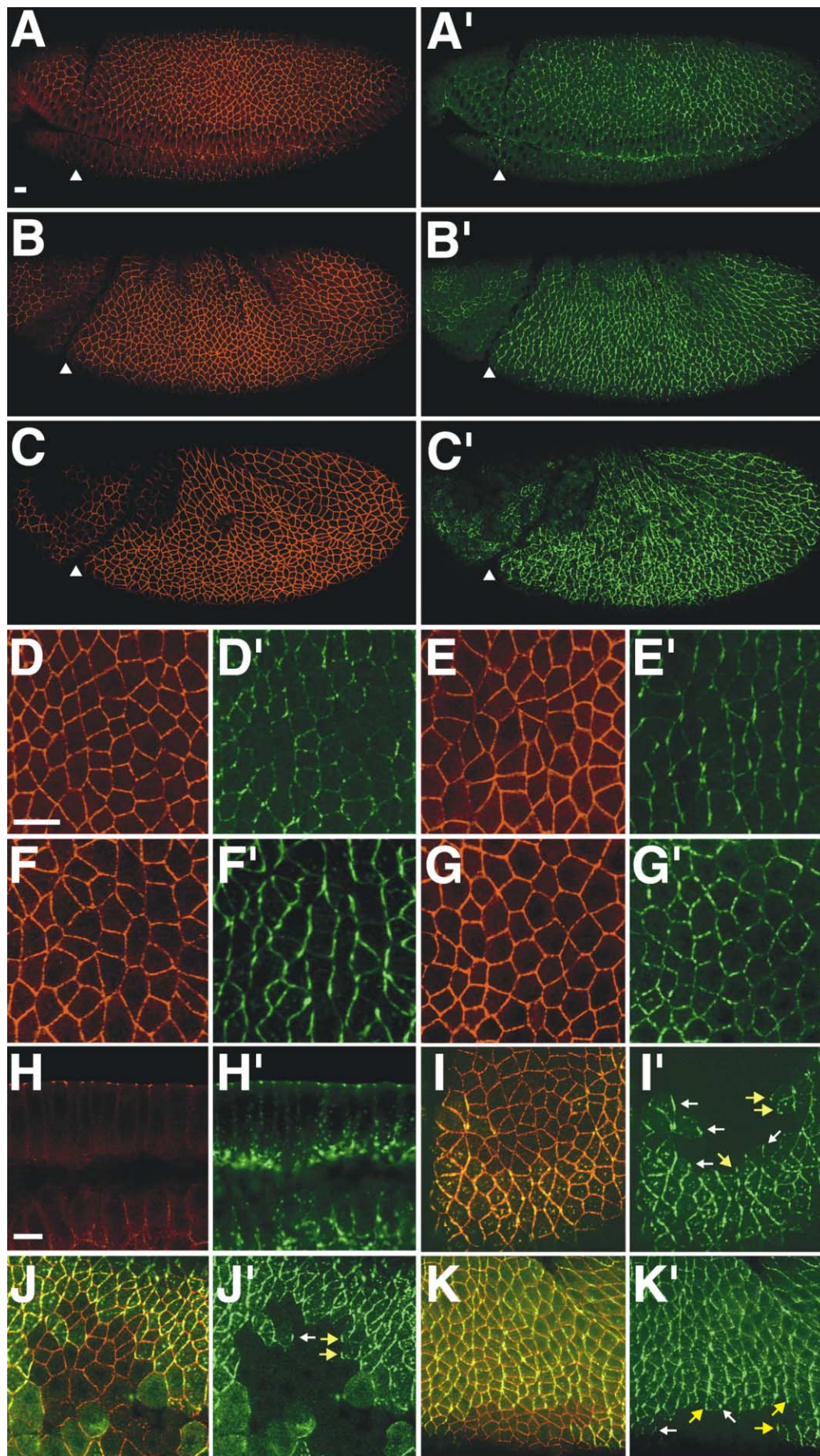
that eliminate dorsal or ventral cell types (Irvine and Wieschaus, 1994). Instead, the patterning of cell fates along the A-P axis, perpendicular to the direction of cell movement, is required for intercalation. For example, the *Even-skipped* (*Eve*) transcription factor is expressed in stripes along the A-P axis, and germband extension is strongly reduced in embryos where *Eve* is either absent or supplied uniformly (Irvine and Wieschaus, 1994). These findings suggest that spatial information provided by striped expression of the *Eve* transcription factor is essential for cell intercalation. However, it is not understood how differences in gene expression along the A-P axis generate polarized cell movement along the D-V axis.

Interestingly, convergent extension in vertebrates relies on components that function to orient polarized cuticular structures in *Drosophila*. *Drosophila* hairs, bristles, and ommatidia align in a common direction through the action of the *Frizzled*- and *Dishevelled*-dependent planar cell polarity (PCP) pathway (Adler, 2002; Mlodzik, 2002). Vertebrate counterparts of PCP proteins are required for convergent extension movements during axis elongation (reviewed in Keller, 2002; Tada et al., 2002; Wallingford et al., 2002). While PCP components are required for the organization of polarized cell movements at the tissue level, little is known about the molecular asymmetries that constitute this polarity at the cellular level and how they influence cell motility.

In some cases, cellular asymmetries along the planar axis are created by the reorganization of components that are normally polarized along the orthogonal apical-basal axis. For example, the multi-PDZ domain protein Bazooka/PAR-3 marks the apical pole of cells that divide asymmetrically along the apical-basal axis (Schober et al., 1999; Wodarz et al., 1999; Roegiers et al., 2001) and a single pole of cells that divide asymmetrically along the planar axis (Etemad-Moghadam et al., 1995; Bellaiche et al., 2001; Roegiers et al., 2001). Bazooka/PAR-3 has been shown to form a complex with the DmPAR-6 PDZ domain protein and the atypical protein kinase C (DaPKC). These components are required for polarization of the *C. elegans* zygote, segregation of cell fate determinants during asymmetric cell division, spindle rotation, and epithelial apical-basal polarity (reviewed in Doe and Bowerman, 2001; Jan and Jan, 2001; Knoblich, 2001; Ohno, 2001). These diverse functions suggest that a common molecular machinery may serve as a basis for the organization of distinct subcellular structures.

Polarized cell movement during convergent extension ultimately derives from the asymmetric localization of proteins that direct cell motility. Interestingly, intercalating cells in the *Drosophila* germband display a polarized localization of the ectopically expressed Slam protein (Lecuit et al., 2002). Here we show that Slam is present in a bipolar distribution that correlates spatially and temporally with intercalary behavior. These observations indicate that Slam can serve as a molecular marker for polarized cell behavior. We find that pair-rule patterning genes expressed in stripes along the A-P axis are necessary for Slam localization and, conversely, that altering

\*Correspondence: jzallen@molbio.princeton.edu



the geometry of their expression is sufficient to reorient Slam polarity. We demonstrate an endogenous planar polarity in intercalating cells manifested by the accumulation of nonmuscle myosin II at A-P cell borders and Bazooka/PAR-3 at D-V cell borders. Moreover, germ-band extension is defective in *bazooka* mutant embryos, supporting a model where molecular polarization of the cell surface is a prerequisite for polarized cell movement. Therefore, differences in gene expression along the A-P axis may direct planar polarity in intercalating cells through the creation of molecularly distinct cell-cell interfaces that differ in migratory potential.

## Results

### Polarized Distribution of the Ectopically Expressed Slam Protein in Intercalating Cells

Cell movement during germ-band extension is oriented along the D-V axis (Irvine and Wieschaus, 1994), suggesting a mechanism that restricts the productive generation of motility to dorsal and ventral cell surfaces. Molecules that are asymmetrically localized during convergent extension may therefore contribute to the spatial regulation of cell motility. Interestingly, intercalating cells in the *Drosophila* germ-band display a polarized localization of the ectopically expressed Slam protein, a novel cytoplasmic factor required for cellularization in the early embryo (Lecuit et al., 2002). While proteins such as Armadillo/ $\beta$ -catenin are uniformly distributed at the cell surface (Figures 1C and 1F), ectopic Slam is enriched in borders between neighboring cells along the A-P axis (Figures 1C' and 1F'). This polarized Slam population is present in a punctate apical distribution (Figure 1H'), coincident with the adherens junction component Armadillo/ $\beta$ -catenin (Figure 1H). Therefore, intercalating cells have distinct apical junctional domains that differ in their capacity for Slam association.

Interestingly, we found that the polarized distribution of ectopic Slam protein is spatially and temporally correlated with intercalary behavior. Slam polarity is not observed in Stage 6 embryos prior to the onset of intercalation (Figures 1A' and 1D'). Slam accumulation at A-P cell borders first appears in late Stage 7 (Figures 1B' and 1E'), when cells of the germ-band initiate intercalation, and reaches its full extent during the period of sustained intercalation in Stage 8 (Figures 1C' and 1F'). In contrast, Slam is uniformly distributed in cells of the head region (Figure 1G') and the dorsal ectoderm (data

not shown), which do not undergo intercalary movements. These results indicate that the polarized distribution of ectopic Slam protein is specific to intercalating cells and that Slam can therefore serve as a molecular marker for the visualization of polarized cell behavior.

### Slam Labels Anterior and Posterior Cell Surfaces in a Bipolar Distribution

The enrichment of Slam at borders between neighboring cells along the A-P axis is consistent with two modes of localization: Slam could mark one side of each cell in a unipolar distribution, or Slam could localize to both anterior and posterior surfaces in a bipolar pattern. To distinguish between these possibilities, we generated mosaic embryos where Slam-expressing cells were juxtaposed with unlabeled cells, using the *Horka* mutation to induce sporadic chromosome loss in early embryos (Szabad et al., 1995). We found that Slam protein accumulates at anterior and posterior boundaries of mosaic clones (Figures 1I–1K), indicating that ectopic Slam protein is targeted to both anterior and posterior surfaces of intercalating cells in a symmetric, bipolar distribution. The bipolar localization of ectopic Slam corresponds well with the bidirectionality of cell movement during germ-band extension, where cells are equally likely to migrate dorsally or ventrally during intercalation (Irvine and Wieschaus, 1994). Bipolar motility is also observed during convergent extension in the presumptive *Xenopus* and *Ciona* notochords and in *Xenopus* neural plate cells in the absence of midline structures (Shih and Keller, 1992; Elul and Keller, 2000; Munro and Odell, 2002).

### A-P Patterning Genes Are Required for Planar Polarity in Intercalating Cells

To extend the spatial and temporal correlation between Slam polarity and cell movement, we asked if this polarized Slam localization is achieved in mutants that are defective for intercalation. Cell intercalation is dependent on the transcriptional cascade that generates cell fates along the A-P axis, in the direction of tissue elongation and perpendicular to the migrations of individual cells (Irvine and Wieschaus, 1994). A-P patterning reflects the hierarchical action of maternal, gap, and pair-rule genes (Schupbach and Wieschaus, 1986; Nüsslein-Volhard et al., 1987). Cell fate differences along the A-P axis are abolished in embryos maternally deficient for the *bicoid*, *nanos*, and *torso-like* genes (referred to as *bicoid nanos torso-like* mutants; Nüsslein-Volhard et al.,

Figure 1. Polarized Distribution of Ectopic Slam Protein in Intercalating Cells

Armadillo/ $\beta$ -catenin (red, [A–K]), Slam (green, [A'–H'] and [I–K]).

(A–G) Lateral views, anterior left and dorsal up. The germ-band is posterior to the cephalic furrow (arrowheads). No Slam polarity is observed in a Stage 6 embryo (A' and D'). Accumulation of Slam at vertical interfaces between cells along the A-P axis first appears in late Stage 7 (B' and E') and becomes pronounced in Stage 8 (C' and F'). Slam polarity is not observed in cells of the head region at Stage 8 (G') which do not undergo intercalation.

(H) Cross-section, apical up, basal down. Slam protein redistributes from a basal location at cellularization (Lecuit et al., 2002) to the apical cell surface in a Stage 8 embryo (H').

(I–K) Lateral views of Stage 8 mosaic embryos, anterior left and dorsal up. Slam (green) is present at both anterior (yellow arrows) and posterior (white arrows) borders of germ-band cells. Polarized cells at clone boundaries were counted in 24 mosaic embryos (2–16 cells scored per mosaic, depending on the length, position, and orientation of the clone boundary). 90/90 polarized cells at posterior clone boundaries localized Slam protein to their exposed anterior surfaces and 91/93 polarized cells at anterior clone boundaries localized Slam protein to their exposed posterior surfaces. Occasional cells with uniform Slam were excluded from this analysis. Scale bars = 10  $\mu$ m.

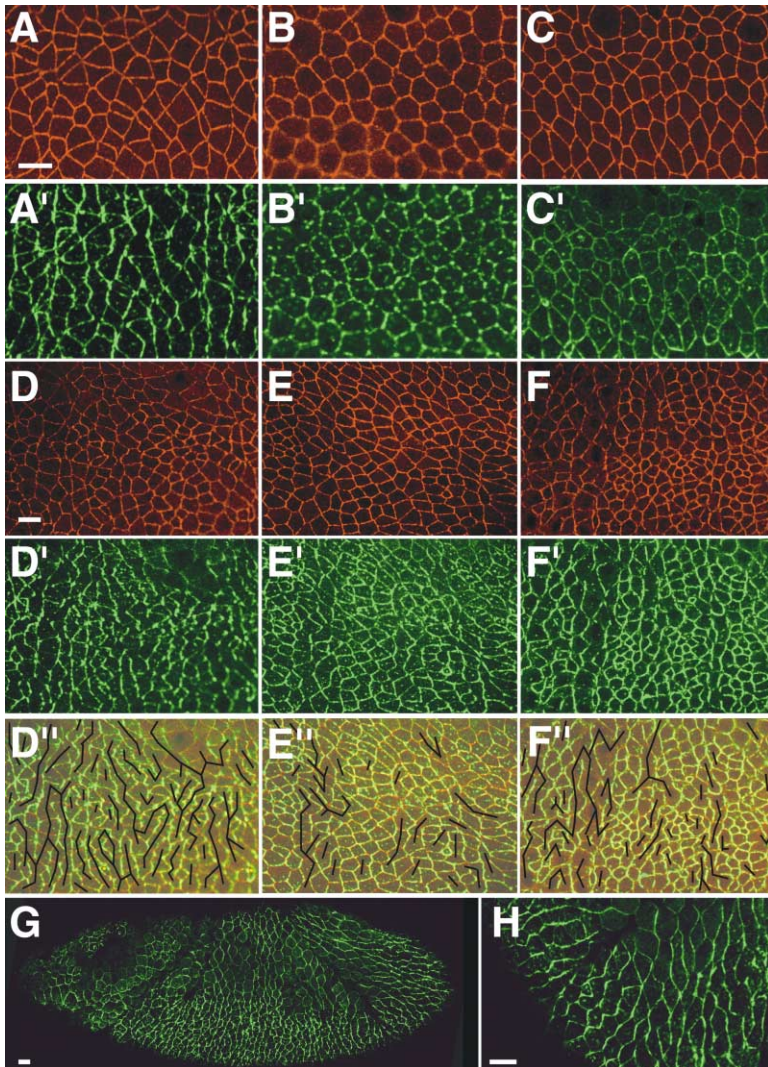


**Figure 2. Slam Polarity Requires A-P Pattern**  
 Armadillo/ $\beta$ -catenin (red, [A–F]), Slam (green, [A'–F'], [G], and [H]), and merge (D''–F''). Lateral views, anterior left and dorsal up.  
 (A) Armadillo is uniform at the apical cell surface in a wild-type embryo (A) while Slam is enriched in vertical interfaces between neighboring cells along the A-P axis (A').  
 (B) Slam is uniform at the apical cell surface in *bicoid nanos torso-like* mutant that lacks A-P pattern.  
 (C) Slam is uniformly distributed in a *knirps hunchback forkhead tailless* mutant that lacks A-P pattern in the germband.  
 (D) Wild-type Slam polarity in an *eve/+* heterozygote (D'). Continuous chains of polarized cells are indicated by black lines in (D'')–(F'').  
 (E) Slam is more uniformly distributed in an *eve* mutant (E'), while rows of polarized cells persist (E'').  
 (F) Occasional Slam polarity in a *runt* mutant (F' and F'').  
 (G and H) Normal Slam polarity in a *dishevelled* germline clone lacking maternal and zygotic Dishevelled protein. Note that Slam polarity correctly shifts around the posterior end of the embryo (anterior left in center of [H] and anterior up at the top left corner). Scale bars = 10  $\mu$ m.

1987), and these mutant embryos do not exhibit intercalary behavior (Irvine and Wieschaus, 1994). We found that ectopic Slam is correctly targeted to the apical cell surface in *bicoid nanos torso-like* mutants, but fails to adopt a polarized distribution in the plane of the epithelium (Figure 2B'; 0/9 mutant embryos exhibited wild-type Slam polarity).

Downstream of the maternal patterning genes, gap genes establish overlapping subdomains along the A-P axis. A quadruple mutant for the gap genes *knirps*, *hunchback*, *forkhead*, and *tailless* lacks A-P pattern within the germband while retaining terminal structures. This quadruple mutant exhibits severely reduced cell intercalation (Irvine and Wieschaus, 1994), and mutant embryos also display a loss of Slam polarity (Figure 2C'; 0/5 *knirps hunchback forkhead tailless* mutants and 12/12 heterozygotes exhibited wild-type Slam polarity). Note that the absence of planar polarity in A-P patterning mutants correlates with a more hexagonal appearance of germband cells (Figures 2B and 2C), in contrast to the irregular morphology of wild-type intercalating cells (Figure 2A).

In response to maternal and gap genes, pair-rule patterning genes expressed in narrow stripes act in combination to assign each cell a distinct fate along the A-P axis (Nüsslein-Volhard et al., 1987). In particular, the *even-skipped* (*eve*) and *runt* pair-rule genes are essential for germband extension (Irvine and Wieschaus, 1994; 27% defective embryos from *runt/+* females and WT males, n = 103; 1/4 are predicted to be hemizygous mutant). This strong requirement for *eve* and *runt* during germband extension contrasts with the more subtle effects in mutants for other pair-rule genes such as *hairy* and *ftz* (Irvine and Wieschaus, 1994). Consistent with these defects in intercalation, *eve* and *runt* mutants also displayed aberrant Slam localization (Figures 2E' and 2F'; 0/10 *eve* mutants, 11/11 *eve/+* heterozygotes, 0/8 *runt* mutants, and 13/13 *runt/+* heterozygotes exhibited wild-type Slam polarity). These results establish a correlation between intercalary behavior and the polarized localization of the ectopic Slam marker.

While *eve* and *runt* mutants fail to complete germband extension, they extend further than embryos lacking maternal and gap genes, suggesting that some intercalary

behavior is retained (Irvine and Wieschaus, 1994). Consistent with this possibility, Slam polarity is only partially disrupted in *eve* and *runt* mutants. While some cells display an aberrant uniform Slam distribution, in other cells Slam is correctly enriched at A-P cell interfaces (black lines, Figure 2E' and 2F'). Therefore, the residual intercalation in *eve* and *runt* mutants correlates with the establishment of planar polarity in a subset of germ-band cells.

#### **Ectopic Eve and Runt Expression Reorients Planar Polarity in Intercalating Cells**

The disruption of Slam polarity in A-P patterning mutants demonstrates that proper gene expression along the A-P axis is required for planar polarity in intercalating cells. In particular, the Eve and Runt transcription factors are expressed in 7 stripes at the onset of germ-band extension and 14 stripes as intercalation proceeds (Frasch and Levine, 1987; Klingler and Gergen, 1993). Each cell in the germ-band is assigned a fate distinct from its anterior and posterior neighbors through the graded and partially overlapping expression of these and other pair-rule genes (Frasch and Levine, 1987; Lawrence and Johnston, 1989; Klingler and Gergen, 1993). Slam preferentially accumulates at contacts between cells with different levels of pair-rule gene activity, suggesting a model where cells concentrate specific proteins at interfaces with neighbors that differ in A-P identity. To directly address this model, we generated mosaic embryos with altered patterns of pair-rule gene expression in order to artificially introduce differences between dorsal and ventral neighbors. We then asked if Slam protein is aberrantly recruited to these ectopic juxtapositions between different cell types, even at interfaces that are perpendicular to the normal axis of polarity.

We used the *Horka* mutation to generate embryos that ectopically express Eve or Runt in a mosaic pattern (Experimental Procedures). When these genes are ubiquitously expressed, planar polarity is generally disrupted and Slam displays a more uniform localization (Figures 3B and 3F). This disruption of Slam polarity correlates with defective germ-band extension in Eve and Runt overexpressing embryos (Irvine and Wieschaus, 1994; 88% defective embryos from *mat $\alpha$ Tub-Gal4VP16 67C;15* females x *UAS-runt* males,  $n = 605$ , versus 1% defective *mat $\alpha$ Tub-Gal4VP16 67C;15* control embryos,  $n = 457$ ). The effects of Eve and Runt overexpression are not mimicked by overexpression of other pair-rule proteins such as Paired, Odd-paired, or Sloppy-paired (Experimental Procedures). Moreover, localized sources of Eve or Runt expression direct aberrant patterns of polarity in mosaic embryos. For example, mosaic embryos display circles of Slam polarity that are bordered by ectopic Eve clones (Figures 3C and 3D; 13 Eve mosaics). Similarly, Slam polarity in germ-band cells is diverted from its normal orientation to follow boundaries of Runt misexpression (Figures 3G and 3H; 10 Runt mosaics). These results demonstrate that ectopic sites of Eve and Runt expression can reorient Slam polarity at clone boundaries, even when these interfaces are perpendicular to the normal axis of polarity.

In contrast to the reorientation of planar polarity at

boundaries of Eve and Runt misexpression, cells distant from the clone often exhibited complex patterns of Slam localization. These patterns may arise from nonautonomous effects of pair-rule gene activity, as well as aberrant cell movements and ectopic folds that form at clone boundaries, suggestive of a disruption in cell adhesion (data not shown). We therefore examined mosaic embryos at Stage 7, prior to the onset of cell movement and ectopic fold formation. While early Stage 7 embryos do not normally exhibit Slam polarity, ectopic Eve induces a precocious accumulation of Slam at clone boundaries (Figure 3E; 6 Eve mosaics). In contrast, ectopic Runt only occasionally induced a subtle polarity at Stage 7 (1 of 3 Runt mosaics). The more potent effect of the *eve* transgene may reflect higher levels of ectopic expression compared to the endogenous *eve* stripes (Figure 3E'). These mosaic experiments indicate that differences in gene expression play an instructive role in the generation of planar polarity in intercalating cells. While Eve and Runt are both sufficient for planar polarity, the absence of either gene alone disrupts polarity (Figure 2). However, the defects in *eve* or *runt* single mutants may result from a combined disruption of multiple pair-rule genes, as loss of *eve* leads to altered *runt* expression and vice versa (Frasch and Levine, 1987; Klingler and Gergen, 1993).

Generation of planar polarity by ectopic Eve expression is subject to the same spatial requirements as in wild-type polarity: Eve clones in the head region failed to induce polarity (6 Eve mosaics), suggesting that these cells are resistant to Eve-dependent polarization. In contrast, ectopic Runt expression in the head led to a concentration of Slam at clone boundaries (Figures 3I and 3J; 7 Runt mosaics), despite the fact that these cells do not normally display Slam polarity (Figure 1G) or intercalary behavior (Irvine and Wieschaus, 1994). These results indicate that in contrast to Eve, Runt can induce planar polarity in head cells, raising the possibility of functional distinctions between Eve and Runt target genes.

#### ***Drosophila* Germ-band Extension Is Independent of Frizzled and Dishevelled**

The Eve and Runt transcription factors ultimately direct Slam polarity and cell intercalation through the transcriptional regulation of target genes. To identify downstream effectors involved in this process, we analyzed components of the noncanonical planar cell polarity (PCP) pathway that is required for convergent extension in vertebrates. We found that germ-band extension occurs normally in the majority of embryos lacking the Frizzled and Frizzled2 receptors (81% of *fz<sup>H51</sup> fz2<sup>C1</sup>* germline clones maternally and zygotically deficient for both proteins,  $n = 27$ ). Similarly, germ-band extension is unaffected in the absence of Dishevelled (100% of *dsh<sup>V26</sup>* germline clones maternally and zygotically deficient for Dishevelled protein,  $n = 76$ ). Moreover, *dishevelled* mutants exhibit a normal polarization of the Slam marker (Figures 2G and 2H; 12/12 *dsh<sup>V26</sup>* germline clones displayed wild-type Slam polarity). These results demonstrate that molecular and behavioral properties of planar polarity in the *Drosophila* germ-band do not require Frizzled or Dishevelled function.

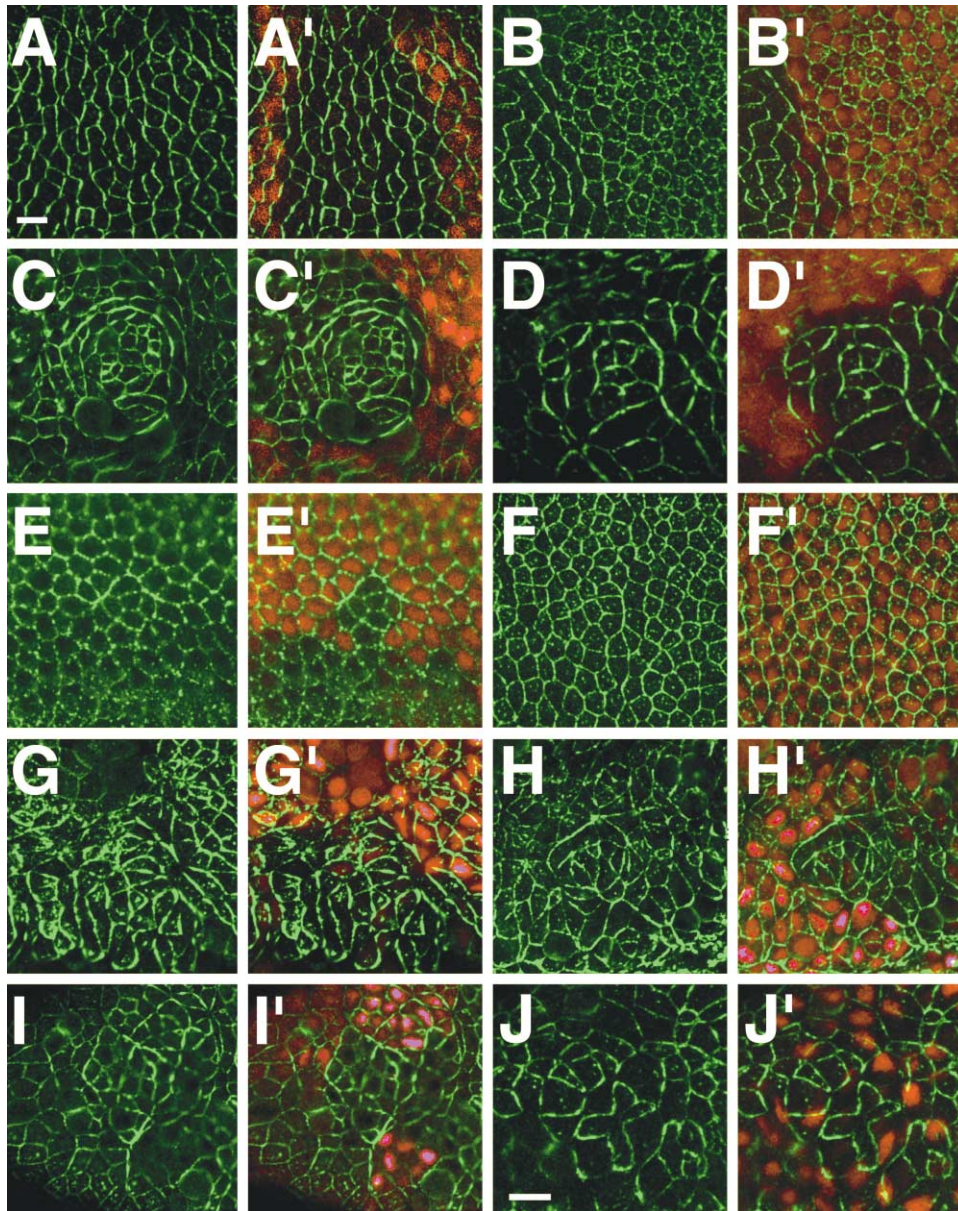


Figure 3. Eve and Runt Expression Orients Planar Polarity in Intercalating Cells

Slam (green, all), Eve (orange, [A'–E']), Runt (orange, [F'–J']). Lateral views, anterior left and dorsal up.

(A) Wild-type Slam polarity in a nonmosaic Stage 8 embryo.

(B) Slam polarity is disrupted in regions of ubiquitous Eve expression, with normal polarity in nonoverexpressing regions (left side of panel).

(C and D) In Stage 8 mosaic embryos, Slam polarity follows boundaries of ectopic Eve expression. Note that this polarity forms a circle beyond the boundary of Eve misexpression.

(E) Precocious Slam polarity at the boundary of ectopic Eve expression in a Stage 7 mosaic embryo. Ectopic Eve (top half of panel) is expressed more strongly than endogenous Eve (bottom half).

(F) Slam polarity is generally disrupted when Runt is ubiquitously expressed in a Stage 8 embryo.

(G and H) Stage 8 mosaic embryos reorient Slam polarity at boundaries of ectopic Runt expression.

(I and J) Ectopic Runt induces Slam polarity in normally unpolarized cells of the head at Stage 8. Scale bars = 10  $\mu$ m.

#### Enrichment of Nonmuscle Myosin II at A-P Interfaces and Bazooka/PAR-3 at D-V Interfaces in Intercalating Cells

The polarized distribution of ectopic Slam in intercalating cells provides the first clue to a molecular distinction between D-V cell interfaces that generate productive cell motility and A-P interfaces that do not. However,

endogenous Slam mRNA and protein are not detected during germband extension (Lecuit et al., 2002; Stein et al., 2002), indicating that Slam may not play a functional role in cell intercalation (see Experimental Procedures). Slam colocalizes with the Zipper nonmuscle myosin II heavy chain subunit during cellularization and when Slam is ectopically expressed at germband extension

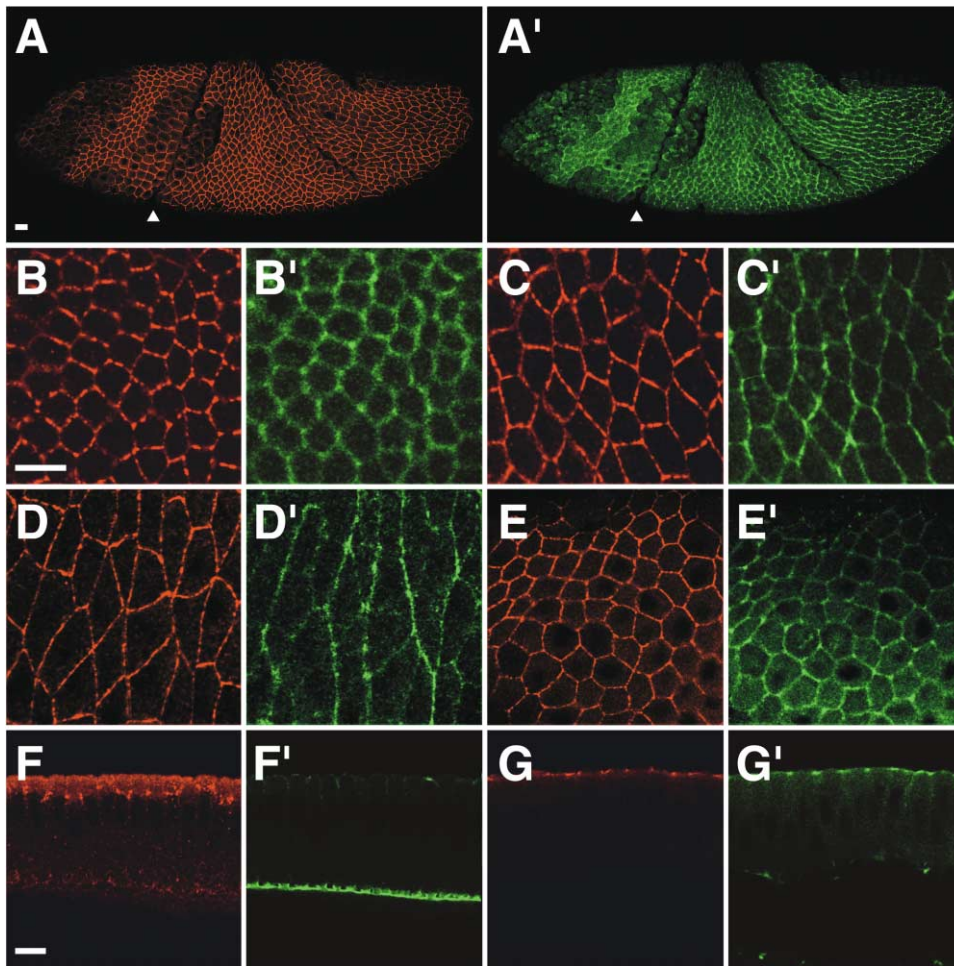


Figure 4. Nonmuscle Myosin II Is Enriched at Borders between Neighboring Cells along the A-P Axis

Armadillo/ $\beta$ -catenin (red, [A–G]), myosin II (green, [A'–G']).

(A–E) Lateral views, anterior left and dorsal up. (A) A Stage 8 embryo showing an accumulation of myosin II (green, [A']) at vertical A-P cell interfaces in the germband epithelium. The germband is posterior to the cephalic furrow (arrowhead).

(B–E) At Stage 6 (B') and Stage 7 (C'), myosin II is approximately uniform at the apical cell surface. (D) Polarized accumulation of myosin II (green) at vertical A-P borders of intercalating cells at Stage 8, in contrast to the more uniformly localized Armadillo/ $\beta$ -catenin (red). (E) Myosin II is uniform in cells of the head region (E'), which do not undergo intercalation.

(F and G) Cross-sections, apical up, basal down. Myosin II is predominantly basal in a Stage 6 embryo (F'), with a subpopulation located apically. This punctate apical localization becomes more pronounced at Stage 8 (G') and colocalizes with the adherens junction component Armadillo/ $\beta$ -catenin (G). Scale bars = 10  $\mu$ m.

(Lecuit et al., 2002). We therefore examined the endogenous distribution of myosin II during germband extension in wild-type embryos. During cell intercalation, myosin II is present in a punctate distribution at the apical cell surface (Figure 4G'), colocalizing with the adherens junction component Armadillo/ $\beta$ -catenin (Figure 4G). In Stage 8 embryos, apical myosin II protein accumulates at interfaces between cells along the A-P axis (Figures 4A' and 4D'; Figure 6). Slam can enhance this polarized localization when ectopically expressed (Lecuit et al., 2002), suggesting that Slam and myosin II may associate with a common localization machinery. Myosin II polarity is not apparent in Stage 6 or early Stage 7 embryos that have not begun intercalation (Figures 4B' and 4C'), indicating that the enrichment of myosin II at A-P interfaces is specific to intercalating cells.

The localized distribution of myosin II (Figure 4) is

not as pronounced as that of ectopic Slam (Figure 1), suggesting that additional asymmetries contribute to the polarization of intercalating cells. To identify such proteins, we examined the localization of components implicated in cell polarity in other cell types. In particular, the PDZ domain protein Bazooka/PAR-3 participates in both apical-basal and planar polarity (reviewed in Doe and Bowerman, 2001; Jan and Jan, 2001; Knoblich, 2001; Ohno, 2001). We found that Bazooka/PAR-3 also exhibits a polarized distribution in intercalating cells. Bazooka, like myosin II, is present in a punctate apical distribution, coincident with the adherens junction component Armadillo/ $\beta$ -catenin (Figure 5I'). However, in contrast to the accumulation of myosin II at A-P cell interfaces, Bazooka is enriched in the reciprocal D-V interfaces (Figures 5A' and 5E'; Figure 6). Bazooka polarity is specific to intercalating cells, where it first

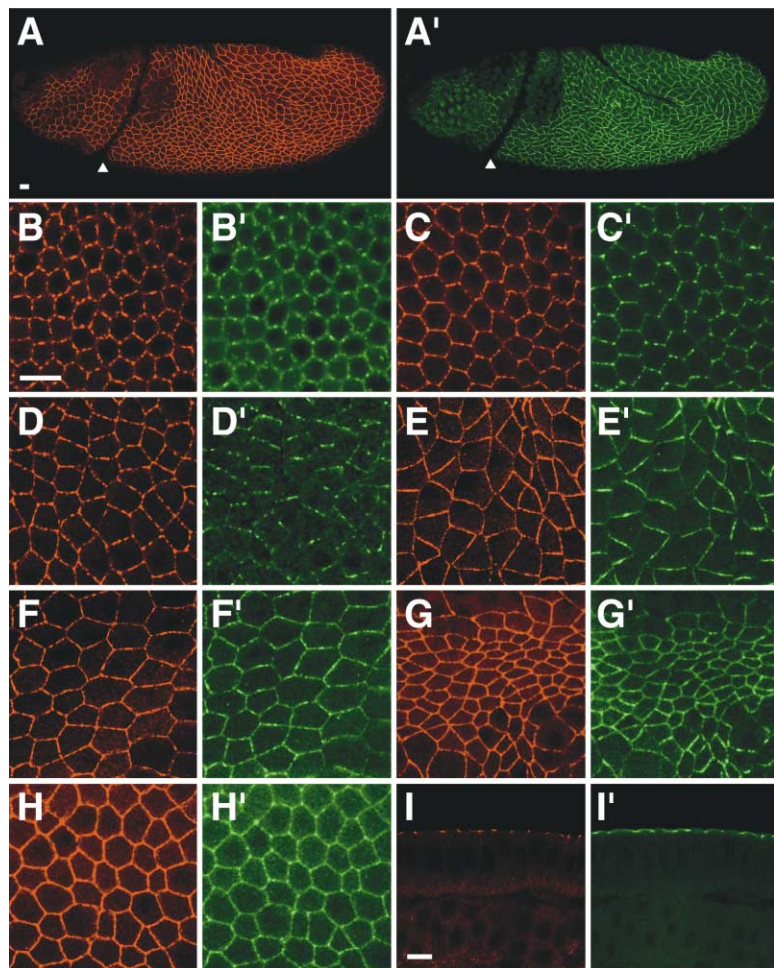


Figure 5. Bazooka/PAR-3 Is Enriched at Borders between Neighboring Cells along the D-V Axis

Armadillo/ $\beta$ -catenin (red, [A–I]), Bazooka (green, [A'–I']).

(A–H) Lateral views, anterior left and dorsal up. (A) Wild-type Stage 8 embryo showing enrichment of Bazooka (green, [A']) at horizontal D-V cell interfaces in the germband epithelium. The germband is posterior to the cephalic furrow (arrowhead). (B–E) At Stage 6 (B') and early Stage 7 (C'), Bazooka is present in a uniform punctate distribution at the apical cell surface. In late Stage 7 (D') and Stage 8 (E'), Bazooka (green) accumulates at horizontal D-V borders in intercalating cells, in contrast to the more uniform localization of Armadillo/ $\beta$ -catenin (red). (F–H) Bazooka is not polarized in cells of the head region (F') which do not undergo intercalation, and in a Stage 9 embryo that has completed germband extension (G'). Bazooka polarity is eliminated in a *bicoid nanos torso-like* mutant that lacks A-P pattern (H').

(I) Cross-section, apical up, basal down. Bazooka (I') colocalizes with Armadillo/ $\beta$ -catenin (I) in apical adherens-type junctions at Stage 8. Scale bars = 10  $\mu$ m.

appears at the onset of intercalary movements in late Stage 7 (Figure 5D'). Bazooka polarity is not observed in cells of the head region that do not undergo intercalation (Figure 5F') and in germband cells following the completion of germband extension at Stage 9 (Figure 5G').

To characterize the relationship between cell shape and the polarized localization of cortical proteins, the orientation of cell borders was measured as an angle relative to the A-P axis (with A-P interfaces closer to 90° and D-V interfaces closer to 0° and 180°). Interfaces from embryos stained for Bazooka and myosin II were ranked according to mean fluorescence intensity as a relative measure of protein distribution (Figure 6B). These results illustrate that Bazooka and myosin II are enriched in distinct sets of cell-cell interfaces that adopt largely nonoverlapping orientations relative to the A-P axis. This quantitation confirms the visual impression from confocal images and demonstrates that the molecular composition of a cell surface domain is a reliable predictor of its orientation within the epithelial cell sheet.

The polarized localization of Bazooka is abolished in the absence of A-P patterning information in *bicoid nanos torso-like* mutant embryos (Figure 5H'; 0/12 *bicoid nanos torso-like* mutants exhibited wild-type Bazooka polarity). We observe a similar disruption of myosin II polarity in A-P patterning mutants (data not shown). The A-P patterning system may therefore mediate cell intercalation through the polarized accumulation of cell

surface-associated proteins. Bazooka participates in a conserved protein complex containing the atypical PKC (DaPKC; Wodarz et al., 2000), and DaPKC is also enriched in D-V cell interfaces during germband extension (data not shown).

#### Bazooka/PAR-3 Is Required for Normal Germband Extension

To ask whether the polarized Bazooka/PAR-3 protein is functionally required for germband extension, we examined homozygous *bazooka* (*baz*) mutant embryos. In zygotic *baz* mutants, residual Bazooka protein persists from maternal stores and is often, but not always, correctly distributed along the apical-basal and planar axes (7/9 *baz* mutants versus 13/14 *baz*<sup>+/+</sup> heterozygotes). Despite this maternal Bazooka contribution, loss of zygotic Bazooka disrupted germband extension (Figure 7E; 28% of progeny from *baz*<sup>YD97/+</sup> females and wild-type males were defective for germband extension, n = 536; 1/4 are predicted to be hemizygous mutant). In wild-type embryos, the posterior end of the extended germband is located at ~70% egg length from the posterior pole (Figure 7B). Of the progeny of *baz*<sup>YD97/+</sup> females and wild-type males, 72% were wild-type-like (extension to  $\geq$ 60% egg length), 25% were partially defective (40%–50% egg length), and 3% were strongly defective ( $\leq$ 30% egg length, n = 536 total). These results

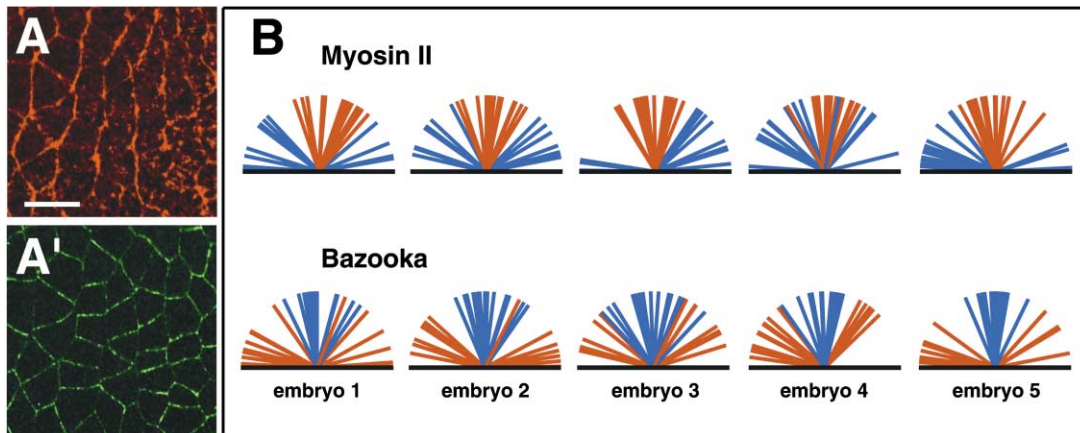


Figure 6. Myosin II and Bazooka Define Reciprocal Cell Surface Domains in Intercalating Cells

Myosin II (red, [A]), Bazooka (green, [A']).

(A) Lateral view, anterior left and dorsal up. Myosin II is enriched in vertical A-P interfaces in intercalating cells (A) and Bazooka/PAR-3 is enriched in horizontal D-V interfaces in the same cells (A'). The angular distribution of these interfaces relative to the A-P axis is graphed in (B), with the most strongly labeled 25% of interfaces shown in red and the most weakly labeled 25% in blue (60 measurements per embryo, each line represents one cell-cell interface). Myosin II (top row) is enriched in interfaces (red) that are oriented at angles closer to 90° relative to the A-P axis (black line) and is depleted from more horizontal interfaces that lie parallel to the A-P axis. In contrast, Bazooka/PAR-3 (bottom row) is enriched in interfaces (red) that are oriented at angles closer to 0° and 180° relative to the A-P axis and is depleted from more vertical interfaces. Scale bar = 10 μm.

demonstrate that Bazooka is required for normal germband extension.

Bazooka/PAR-3 and the associated DmPAR-6 and DaPKC components also influence epithelial cell polarity along the apical-basal axis (Muller and Wieschaus, 1996; Wodarz et al., 2000; Petronczki and Knoblich, 2001). To address the possibility that germband extension defects may occur indirectly as a result of disrupted apical-basal polarity, we analyzed properties of apical-basal polarity in zygotic *baz* mutants, where some functions are carried out by maternal gene products (Wieschaus and Noell, 1986). Zygotic *baz* mutant embryos exhibit several signs of normal apical-basal polarity at gastrulation, including a monolayer epithelial morphology in the germband (Figure 7F), and the correct distribution of proteins to apical and lateral membrane domains (Figure 7F'; 20/20 *baz* mutants). This is consistent with previous findings that zygotic *baz* mutants exhibit proper localization of the Armadillo/β-catenin adherens junction component prior to Stage 10 of embryogenesis (Muller and Wieschaus, 1996). These results demonstrate that properties of apical-basal polarity are established correctly in *baz* mutant embryos during germband extension, consistent with a direct role for Bazooka in cell movements along the planar axis, independent of its later effects on apical-basal polarity.

## Discussion

The organization of cell fates has a dramatic effect on morphogenetic movements, but it is not understood how cell behavior is generated downstream of cell fate determination. In particular, differences in gene expression along the A-P axis are essential for polarized cell motility during *Drosophila* germband extension (Irvine and Wieschaus, 1994). Here, we show that A-P patterning genes also promote the polarized distribution of cortical proteins, suggesting a molecular basis for their

effect on cell behavior. The ectopically expressed Slam marker preferentially localizes to sites of cell-cell contact along the A-P axis (Lecuit et al., 2002), and we found that Slam is distributed in a bipolar pattern that correlates spatially and temporally with cell movement. This polarity is disrupted in A-P patterning mutants that are defective for intercalation. Specifically, the *eve* and *runt* pair-rule genes are normally expressed in stripes along the A-P axis and Slam polarity is disrupted when these genes are either absent or uniformly expressed. Moreover, ectopic *Eve* and *Runt* expression is sufficient to reorient planar polarity in mosaic embryos. Therefore, global patterns of *Eve* and *Runt* expression provide spatial information that coordinates planar polarity across a multicellular population.

The local reorientation of planar polarity in response to *Eve* and *Runt* expression argues that planar polarity is generated by cell-cell interactions, rather than a distant polarizing cue. In addition to these local effects of *Eve* and *Runt* on planar polarity, Slam polarity frequently adopted a circular pattern in mosaic embryos, even when *Eve* and *Runt* were not present along the entire circumference of the circle. This unexpected configuration indicates that polarizing information can propagate from cell to cell downstream of an *Eve*-dependent signal. A similar relay mechanism is suggested by the swirling patterns of wing hair polarity that persist in *Drosophila* mutants defective for the PCP signaling pathway (Adler, 2002). Therefore, mechanisms of cell-cell communication may reinforce local polarizing events in the organization of a two-dimensional cell population.

## Cell Surface Domains Enriched for Bazooka/PAR-3 or Nonmuscle Myosin II May Influence Polarized Cell Movement

We demonstrate that intercalating cells display a polarized accumulation of nonmuscle myosin II at A-P cell borders and Bazooka/PAR-3 at D-V borders. Moreover,

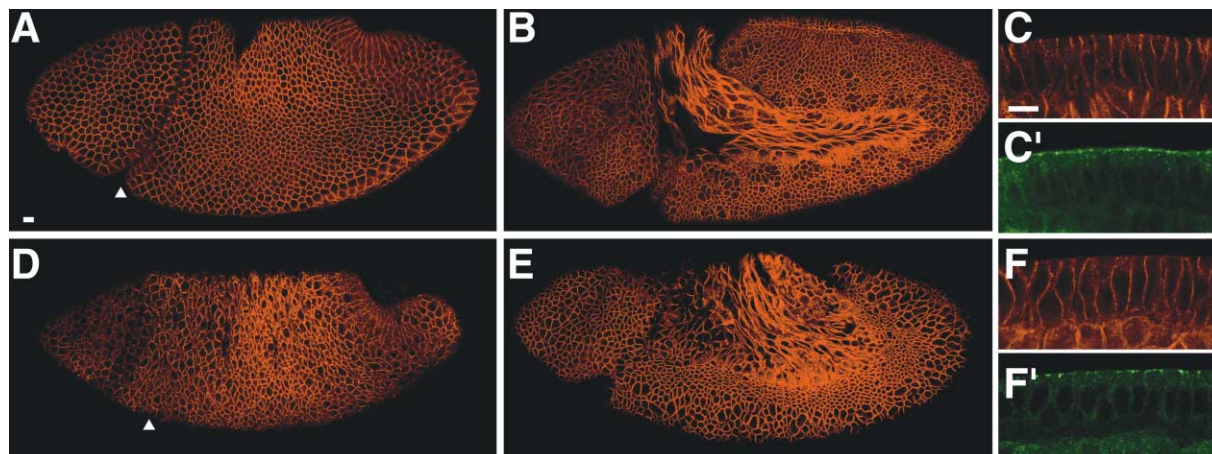


Figure 7. Bazooka Is Required for Germband Extension

Neurotactin (red, [A–F]) and Bazooka (green, [C' and F']).

(A, B, D, and E) Lateral views, anterior left and dorsal up. (C and F) Cross-sections, apical up, basal down. The germband is posterior to the cephalic furrow (arrowheads).

(A and B) A *baz*<sup>+/+</sup> heterozygote exhibits normal morphology at the onset of germband extension ([A], late Stage 7) and at the fully extended germband stage ([B], Stage 9).

(C) Wild-type distribution of Neurotactin at lateral cell surfaces (C) and Bazooka at apical junctions (C') in a *baz*<sup>+/+</sup> heterozygote.

(D and E) A *baz* zygotic mutant initiates germband extension ([D], late Stage 7) but fails to fully elongate ([E], Stage 9).

(F) Properties of apical-basal polarity are preserved in *baz* zygotic mutants, such as the lateral distribution of neurotactin (F) and apical localization of maternal Bazooka protein (F'). Scale bars = 10  $\mu$ m.

germband extension is disrupted in zygotic *baz* mutants, supporting the hypothesis that this polarized protein localization is important for cell movement. While Bazooka can also affect cell polarity along the apical-basal axis, germband extension occurs normally in zygotic mutants for other components that are required for apical-basal polarity at early (*crumbs* and *stardust*) or late (*discs large*, *scribbles*, and *lethal giant larvae*) embryonic stages (data not shown), suggesting that zygotic apical-basal polarity mutants do not generally disrupt intercalation.

The formation of cell surface domains enriched for Bazooka or myosin II could occur independently or in a sequential fashion. In *C. elegans*, the myosin II subunits NMY-2 and MLC-4 are required to localize the Bazooka homolog PAR-3 to the anterior cortex of the 1-cell embryo (Etemad-Moghadam et al., 1995; Guo and Kemphues, 1996; Shelton et al., 1999). In contrast, in dividing *Drosophila* neuroblasts myosin II appears to function at a later step, subsequent to Bazooka localization (Barros et al., 2003). Bazooka and myosin II colocalize with Armadillo/ $\beta$ -catenin in adherens-type spot junctions that are precursors of the mature zonula adherens (Muller and Wieschaus, 1996), indicating that adherens junctions may provide a focal point for the regulation of polarized motility in epithelial cells. However, Bazooka/PAR-3 and myosin II polarity at the apical cell surface may also occur in response to motile behavior initiated elsewhere in the cell, as basolateral protrusions are observed during convergent extension in other epithelial tissues (Hardin, 1989; Munro and Odell, 2002).

Alternatively, myosin II and Bazooka/PAR-3 could play a direct role in polarized cell movement through the regulation of cell motility, contractility, or adhesion. Myosin II at nonmigratory A-P surfaces of intercalating

cells could function to inhibit lamellipodia formation (Katsumi et al., 2002) or downregulate adherens junctions (Sahai and Marshall, 2002). Conversely, Bazooka may function to promote motility at migratory D-V surfaces, as Bazooka/PAR-3 induces protrusive activity in cultured mammalian epithelial cells (Mishima et al., 2002) and localizes to leading edge extensions of migrating border cells in *Drosophila* oogenesis (Abdelilah-Seyfried et al., 2003). Therefore, Bazooka/PAR-3 and myosin II may carry out spatially restricted functions that directly influence cell movement.

A third possibility is that reciprocal cell surface domains enriched for myosin II or Bazooka/PAR-3 could serve as a scaffold for the differential recruitment of effector proteins. The diverse effects of Bazooka and its associated DmPAR-6 and DaPKC proteins on polarity in epithelia and dividing cells raise the possibility that a common set of components may polarize distinct subcellular structures by recruiting different effectors. In asymmetrically dividing neuroblasts, Bazooka is required for the localization of Numb, Pon, Miranda, and Prospero to the basal side of the cell. Similarly, *C. elegans* PAR-3 is required for the distribution of PAR-1, PAR-2, and MEX-5 to restricted subcellular domains (reviewed in Doe and Bowerman, 2001; Jan and Jan, 2001; Knoblich, 2001; Ohno, 2001).

#### Local Cell-Cell Interactions Provide Spatial Cues that Direct Planar Polarity

While components required for planar cell polarity have been identified (reviewed in Adler, 2002; Keller, 2002; Mlodzik, 2002; Tada et al., 2002; Wallingford et al., 2002), little is known about the extracellular cues that orient this polarity across a multicellular population. For example, the organization of *Drosophila* wing hairs depends

on the Frizzled receptor, but an extracellular ligand that aligns these hairs in a common direction has not been identified. The secreted Wnt11 ligand is required for convergent extension in vertebrates, but can function when expressed uniformly (Heisenberg et al., 2000; Tada and Smith, 2000), indicating that spatial information is not provided by localized Wnt11 expression. Here, we show that planar polarity in *Drosophila* germband extension is locally established through the concentration of specific proteins at sites of contact between cells with different levels of Eve and Runt expression. Cells could monitor the identity of their neighbors through qualitative or quantitative differences in the activity of cell surface proteins, perhaps through ligand-receptor mediated signaling events or adhesion-based cell sorting (Wieschaus et al., 1991; Steinberg and Takeichi, 1994). Transcriptional targets of Eve and Runt are therefore likely to include components that mediate intercellular signaling events involved in the transmission of polarizing information during multicellular reorganization.

#### Experimental Procedures

##### Fly Stocks and Genetics

Flies were maintained by standard methods at 20–21°C, unless otherwise noted. HA-tagged Slam protein was ectopically expressed using the *UAS-slamHA12* (X) and *UAS-slamHA16* (II) transgenes (Lecuit et al., 2002) and the *mat $\alpha$ Tub-Gal4VP16 67C;15* driver (gift of D. St. Johnston). Germline clones for *dsh* and *fz fz2* were generated using the FLP-DFS system (Chou and Perrimon, 1992). The *bicoid nanos torso-like* mutant is female sterile, and A-P patterning-deficient embryos were obtained as progeny of homozygous females. All other mutants represent a loss of zygotic gene function. *dsh* and *fz fz2* germline clones were retroactively genotyped by the mutant cuticle phenotype. Fixed embryos were genotyped by absence of sex lethal expression (*dsh*), absence of lacZ expression (*baz*), or altered *eve* and *runt* expression (A-P patterning mutants). The following mutant crosses were conducted: *mat $\alpha$ Tub-Gal4VP16 67C; bicoid<sup>E1</sup> nanos<sup>L7</sup> torso-like<sup>146</sup>* females x *UAS-slamHA16* males; *mat $\alpha$ Tub-Gal4VP16 67C; knirps<sup>ID48</sup> hunchback<sup>7M48</sup> forkhead<sup>E200</sup> tailless<sup>L10</sup>/TM3* females x *UAS-slamHA12*; *knirps<sup>ID48</sup> hunchback<sup>7M48</sup> forkhead<sup>E200</sup> tailless<sup>L10</sup>/+* males; *runt<sup>LB5</sup>/FM7, ftz-lacZ; mat $\alpha$ Tub-Gal4VP16 67C* females x *UAS-slamHA16* males; *eve<sup>R13</sup>/mat $\alpha$ Tub-Gal4VP16 67C; mat $\alpha$ Tub-Gal4VP16 15/+* females x *UAS-slamHA12*; *eve<sup>R13</sup>/+* males; *y w dsh<sup>V26</sup> FRT18D/ovo<sup>D1</sup> FRT18D; mat $\alpha$ Tub-Gal4VP16 67C/hs-FLP* females x *UAS-slamHA16* males; *y w hs-FLP/+; fz<sup>H51</sup> fz2<sup>C1</sup> FRT2A/ovo<sup>D1</sup> FRT2A* females x *fz<sup>H51</sup> fz2<sup>C1</sup> FRT2A/TM3,hb-lacZ* males; *baz<sup>YD97</sup>/FM7,ftz-lacZ* females x *FM7,ftz-lacZ* males.

##### Germband Extension Analysis

Germband extension was scored in living embryos under halocarbon oil (Sigma) at 20–21°C (Slam overexpression and germline clones) or 25°C (*baz*). Embryos were staged according to Wieschaus and Nüsslein-Volhard (1986). The extent of elongation was determined using morphological markers for the anterior (cephalic furrow) and posterior (posterior midgut) limits of the germband. Germband extension is not significantly disrupted by Slam overexpression: 1% defective control embryos from the *mat $\alpha$ Tub-Gal4VP16 67C;15* stock, *n* = 457; 10% defective embryos from Gal4 females x *UAS-SlamHA16* males, *n* = 222; 5% defective embryos from Gal4 females x *UAS-SlamHA12* males, *n* = 251. This same Gal4 driver was used to overexpress pair-rule genes: 11% defective embryos from Gal4 females x *UAS-Prd* males, *n* = 250; 36% defective embryos from Gal4 females x *UAS-Opa* males, *n* = 589; 16% defective embryos from Gal4 females x *UAS-Slp* males, *n* = 366.

##### Immunocytochemistry

Embryos were heat-methanol fixed as described (Muller and Wieschaus, 1996) for staining with the following antibodies: rat anti-HA (1:1000, Roche), mouse anti-Armadillo (1:75, N2-7A1 Developmental Studies Hybridoma Bank, DSHB), guinea pig anti-Eve and

anti-Runt (1:500, gifts of C. Alonso and J. Reintz; Kosman et al., 1998), rabbit and rat anti-Bazooka (1:500; gifts of A. Wodarz; Wodarz et al., 1999), and rabbit anti-myosin II (Zipper myosin II heavy chain, 1:1250, gift of C. Field). Embryos were fixed for 20 min in 3.7% formaldehyde/PBS:heptane and devitellinized in heptane:methanol for staining with the following antibodies: rabbit anti- $\beta$ -gal (1:1000, Cappel), mouse anti- $\beta$ -gal (1:50, DSHB), mouse anti-Neurotactin (1:200, BP106 concentrated, DSHB), mouse anti-Sex lethal (1:10, M-14, DSHB), and rat anti-HA. Secondary antibodies were conjugated with Alexa-488, Alexa-546 (Molecular Probes), or biotin (Vector) followed by Cy5-streptavidin (Jackson Immunoresearch). Embryos were mounted in AquaPolymount (Polysciences, Inc.). Images were obtained on a Zeiss LSM 510 confocal microscope and assembled using Adobe Photoshop and Illustrator software.

##### Mosaic Analysis

Mosaics were generated using the *Horka* mutation to induce sporadic loss of paternally derived chromosomes (Szabad et al., 1995) in embryos that carry paternal *UAS-slamHA* (Figure 1), *UAS-eve* (Figure 3), or *UAS-runt* (Figure 3; Vander Zwan et al., 2003). Ectopic expression was driven by the maternal *mat $\alpha$ Tub-Gal4VP16 67C;15* driver. Mosaic boundaries were defined by cytoplasmic expression of a linked *UAS-nullo $\Delta$ MP-HA* transgene (Hunter et al., 2002; Figure 1) or nonuniform *eve* or *runt* expression (Figure 3). Arm was used as a control to label the cell surface (data not shown). The following crosses were conducted: *mat $\alpha$ Tub-Gal4VP16 67C;15* females x *UAS-slamHA12 UAS-nullo $\Delta$ MP-HA; Horka/+* males; *UAS-slamHA12/+; mat $\alpha$ Tub-Gal4VP16 67C/+; mat $\alpha$ Tub-Gal4VP16 15/+* females x *UAS-eve/+; Horka/+* males; *mat $\alpha$ Tub-Gal4VP16 67C/UAS-slamHA16; mat $\alpha$ Tub-Gal4VP16 15/+* females x *UAS-eve/+; Horka/+* males; *UAS-slamHA12/+; mat $\alpha$ Tub-Gal4VP16 67C/+; mat $\alpha$ Tub-Gal4VP16 15/+* females x *UAS-runt/+; Horka/+* males; *mat $\alpha$ Tub-Gal4VP16 67C/UAS-slamHA16; mat $\alpha$ Tub-Gal4VP16 15/+* females x *UAS-runt/+; Horka/+* males.

##### Quantitation

The distribution of myosin II and Bazooka/PAR-3 in intercalating cells was quantified using Object-Image software to determine the mean fluorescence intensity of each cell-cell interface (using a freely drawn line) and the angle of each interface relative to the A-P axis (using a straight line between the same endpoints). Embryos were labeled with antibodies to both proteins and 60 interfaces counted from a 50  $\mu$ m<sup>2</sup> region, *n* = 5 embryos at Stage 8. Graphic presentations constructed in Adobe Illustrator.

##### Acknowledgments

We are grateful to Chris Field, Andreas Wodarz, Carlos Alonso, and John Reintz for generously providing antibodies; Natalie Deneff, Arno Müller, Cori Bargmann, Ali Nouri, Mimi Shirasu-Hiza, and Richard Zallen for helpful discussions and comments on the manuscript; Joe Goodhouse for advice on confocal microscopy; and Reba Samanta for technical assistance. Some stocks were obtained from the Bloomington *Drosophila* Stock Center. E.W. is an Investigator of the Howard Hughes Medical Institute. J.A.Z. received support from the Damon Runyon Cancer Research Fund and is supported by a Burroughs Wellcome Fund Career Award in the Biomedical Sciences.

Received: November 21, 2003

Revised: January 7, 2004

Accepted: January 9, 2004

Published: March 15, 2004

##### References

- Abdelilah-Seyfried, S., Cox, D.N., and Jan, Y.N. (2003). Bazooka is a permissive factor for the invasive behavior of discs large tumor cells in *Drosophila* ovarian follicular epithelia. *Development* 130, 1927–1935.
- Adler, P.N. (2002). Planar signaling and morphogenesis in *Drosophila*. *Dev. Cell* 2, 525–535.

- Barros, C.S., Phelps, C.B., and Brand, A.H. (2003). *Drosophila* non-muscle myosin II promotes the asymmetric segregation of cell fate determinants by cortical exclusion rather than active transport. *Dev. Cell* 5, 829–840.
- Bellaïche, Y., Radovic, A., Woods, D.F., Hough, C.D., Parmentier, M.-L., O’Kane, C.J., Bryant, P.J., and Schweisguth, F. (2001). The Partner of Inscuteable/Discs-large complex is required to establish planar polarity during asymmetric cell division in *Drosophila*. *Cell* 106, 355–366.
- Campos-Ortega, J.A., and Hartenstein, V. (1985). *The Embryonic Development of Drosophila melanogaster*. (Berlin: Springer-Verlag).
- Chou, T.B., and Perrimon, N. (1992). Use of a yeast site-specific recombinase to produce female germline chimeras in *Drosophila*. *Genetics* 131, 643–653.
- Doe, C.Q., and Bowerman, B. (2001). Asymmetric cell division: fly neuroblast meets worm zygote. *Curr. Opin. Cell Biol.* 13, 68–75.
- Edgar, B.A., and O’Farrell, P.H. (1989). Genetic control of cell division patterns in the *Drosophila* embryo. *Cell* 57, 177–187.
- Elul, T., and Keller, R. (2000). Monopolar protrusive activity: a new morphogenic cell behavior in the neural plate dependent on vertical interactions with the mesoderm in *Xenopus*. *Dev. Biol.* 224, 3–19.
- Etemad-Moghadam, B., Guo, S., and Kemphues, K.J. (1995). Asymmetrically distributed PAR-3 protein contributes to cell polarity and spindle alignment in early *C. elegans* embryos. *Cell* 83, 743–752.
- Frasch, M., and Levine, M. (1987). Complementary patterns of *even-skipped* and *fushi tarazu* expression involve their differential regulation by a common set of segmentation genes in *Drosophila*. *Genes Dev.* 1, 981–995.
- Guo, S., and Kemphues, K.J. (1996). A non-muscle myosin is required for embryonic polarity in *Caenorhabditis elegans*. *Nature* 382, 455–458.
- Hardin, J. (1989). Local shifts in position and polarized motility drive cell rearrangement during sea urchin gastrulation. *Dev. Biol.* 136, 430–445.
- Heisenberg, C.P., Tada, M., Rauch, G.J., Saude, L., Concha, M.L., Geisler, R., Stemple, D.L., Smith, J.C., and Wilson, S.W. (2000). Silberblick/Wnt11 mediates convergent extension movements during zebrafish gastrulation. *Nature* 405, 76–81.
- Hunter, C., Sung, P., Schejter, E.D., and Wieschaus, E. (2002). Conserved domains of the nullo protein required for cell-surface localization and formation of adherens junctions. *Mol. Biol. Cell* 13, 146–157.
- Irvine, K.D., and Wieschaus, E. (1994). Cell intercalation during *Drosophila* germband extension and its regulation by pair-rule segmentation genes. *Development* 120, 827–841.
- Jan, Y.N., and Jan, L.Y. (2001). Asymmetric cell division in the *Drosophila* nervous system. *Nat. Rev. Neurosci.* 2, 772–779.
- Katsumi, A., Milanini, J., Kiosses, W.B., del Pozo, M.A., Kaunas, R., Chien, S., Hahn, K.M., and Schwartz, M.A. (2002). Effects of cell tension on the small GTPase Rac. *J. Cell Biol.* 158, 153–164.
- Keller, R. (2002). Shaping the vertebrate body plan by polarized embryonic cell movements. *Science* 298, 1950–1954.
- Keller, R., Davidson, L., Edlund, A., Elul, T., Ezin, M., Shook, D., and Skoglund, P. (2000). Mechanisms of convergence and extension by cell intercalation. *Philos. Trans. R. Soc. Lond. B Biol. Sci.* 355, 897–922.
- Klingler, M., and Gergen, J.P. (1993). Regulation of *runt* transcription by *Drosophila* segmentation genes. *Mech. Dev.* 43, 3–19.
- Knoblich, J.A. (2001). Asymmetric cell division during animal development. *Nat. Rev. Mol. Cell Biol.* 2, 11–20.
- Kosman, D., Small, S., and Reinitz, J. (1998). Rapid preparation of a panel of polyclonal antibodies to *Drosophila* segmentation proteins. *Dev. Genes Evol.* 208, 290–294.
- Lawrence, P.A., and Johnston, P. (1989). Pattern formation in the *Drosophila* embryo: allocation of cells to parasegments by *even-skipped* and *fushi tarazu*. *Development* 105, 761–767.
- Lecuit, T., Samanta, R., and Wieschaus, E. (2002). *Slam* encodes a developmental regulator of polarized membrane growth during cleavage of the *Drosophila* embryo. *Dev. Cell* 2, 425–436.
- Mishima, A., Suzuki, A., Enaka, M., Hirose, T., Mizuno, K., Ohnishi, T., Mohri, H., Ishigatsubo, Y., and Ohno, S. (2002). Over-expression of PAR-3 suppresses contact-mediated inhibition of cell migration in MDCK cells. *Genes Cells* 7, 581–596.
- Mlodzik, M. (2002). Planar cell polarization: do the same mechanisms regulate *Drosophila* tissue polarity and vertebrate gastrulation? *Trends Genet.* 18, 564–571.
- Muller, H.A., and Wieschaus, E. (1996). Armadillo, Bazooka and Stardust are critical for early stages in formation of the zonula adherens and maintenance of the polarized blastoderm epithelium in *Drosophila*. *J. Cell Biol.* 134, 149–163.
- Munro, E.M., and Odell, G.M. (2002). Polarized basolateral cell motility underlies invagination and convergent extension of the ascidian notochord. *Development* 129, 13–24.
- Nüsslein-Volhard, C., Frohnhof, H.G., and Lehmann, R. (1987). Determination of anteroposterior polarity in *Drosophila*. *Science* 238, 1675–1681.
- Ohno, S. (2001). Intercellular junctions and cellular polarity: the PAR-aPKC complex, a conserved core cassette playing fundamental roles in cell polarity. *Curr. Opin. Cell Biol.* 13, 641–648.
- Petronczki, M., and Knoblich, J.A. (2001). DmPAR-6 directs epithelial polarity and asymmetric cell division of neuroblasts in *Drosophila*. *Nat. Cell Biol.* 3, 43–49.
- Roegiers, F., Younger-Shepherd, S., Jan, L.Y., and Jan, Y.N. (2001). Bazooka is required for localization of determinants and controlling proliferation in the sensory organ precursor cell lineage in *Drosophila*. *Proc. Natl. Acad. Sci. USA* 98, 14469–14474.
- Sahai, E., and Marshall, C.J. (2002). ROCK and Dia have opposing effects on adherens junctions downstream of Rho. *Nat. Cell Biol.* 4, 408–415.
- Schober, M., Schaefer, M., and Knoblich, J.A. (1999). Bazooka recruits Inscuteable to orient asymmetric cell divisions in *Drosophila* neuroblasts. *Nature* 402, 548–551.
- Schupbach, T., and Wieschaus, E. (1986). Germline autonomy of maternal-effect mutations altering the embryonic body pattern of *Drosophila*. *Dev. Biol.* 113, 443–448.
- Shelton, C.A., Carter, J.C., Ellis, G.C., and Bowerman, B. (1999). The nonmuscle myosin II regulatory light chain *mlc-4* is required for cytokinesis, anterior-posterior polarity, and body morphology during *Caenorhabditis elegans* embryogenesis. *J. Cell Biol.* 146, 439–451.
- Shih, J., and Keller, R. (1992). Cell motility driving mediolateral intercalation in explants of *Xenopus laevis*. *Development* 116, 901–914.
- Stein, J.A., Brohier, H.T., Moore, L.A., and Lehmann, R. (2002). Slow as molasses is required for polarized membrane growth and germ cell migration in *Drosophila*. *Development* 129, 3925–3934.
- Steinberg, M.S., and Takeichi, M. (1994). Experimental specification of cell sorting, tissue spreading, and specific spatial patterning by quantitative differences in cadherin expression. *Proc. Natl. Acad. Sci. USA* 91, 206–209.
- Szabad, J., Mathe, E., and Puro, J. (1995). *Horka*, a dominant mutation of *Drosophila*, induces nondisjunction and, through paternal effect, chromosome loss and genetic mosaics. *Genetics* 139, 1585–1599.
- Tada, M., Concha, M.L., and Heisenberg, C.P. (2002). Non-canonical Wnt signalling and regulation of gastrulation movements. *Semin. Cell Dev. Biol.* 13, 251–260.
- Tada, M., and Smith, J.C. (2000). XWnt11 is a target of *Xenopus* Brachyury: Regulation of gastrulation movements via Dishevelled, but not through the canonical Wnt pathway. *Development* 127, 2227–2238.
- Vander Zwan, C.J., Wheeler, J.C., Li, L.-H., Tracey, W.D., Jr., and Gergen, J.P. (2003). A DNA-binding-independent pathway of repression by the *Drosophila* Runt protein. *Blood Cells Mol. Dis.* 30, 207–222.
- Wallingford, J.B., Fraser, S.E., and Harland, R.M. (2002). Convergent

extension: the molecular control of polarized cell movement during embryonic development. *Dev. Cell* 2, 695–706.

Wieschaus, E., and Noell, E. (1986). Specificity of embryonic lethal mutations in *Drosophila* analyzed in germ line clones. *Roux Arch. Dev. Biol.* 195, 63–73.

Wieschaus, E., and Nüsslein-Volhard, C. (1986). Looking at embryos. In *Drosophila. A practical approach*, D.B. Roberts, ed. (Oxford: IRL Press), pp. 199–227.

Wieschaus, E., Sweeton, D., and Costa, M. (1991). Convergence and extension during germband elongation in *Drosophila* embryos. In *Gastrulation*, R. Keller, ed. (New York: Plenum Press), pp. 213–223.

Wodarz, A., Ramrath, A., Kuchinke, U., and Knust, E. (1999). Bazooka provides an apical cue for Inscuteable localization in *Drosophila* neuroblasts. *Nature* 402, 544–547.

Wodarz, A., Ramrath, A., Grimm, A., and Knust, E. (2000). *Drosophila* atypical protein kinase C associates with Bazooka and controls polarity of epithelia and neuroblasts. *J. Cell Biol.* 150, 1361–1374.